ChemComm

Accepted Manuscript

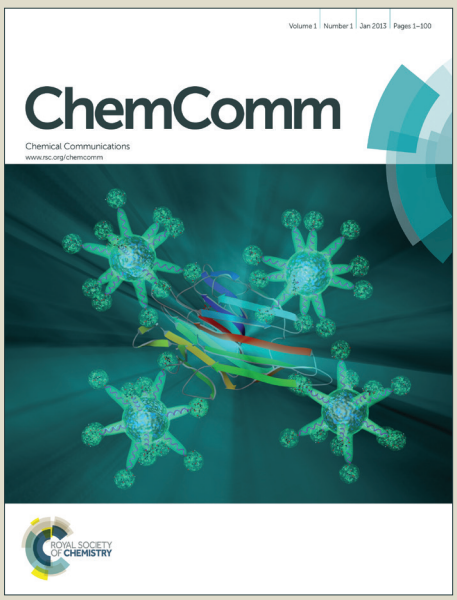

ROYAL SOCIETY OF CHEMISTRY

www.rsc.org/chemcomm

ChemComm

COMMUNICATION

Unprecedented J-Aggregate Formation of Rhodamine Induced by 9-Phenylanthracenyl Substitution†

Received 00th January 20xx,
Accepted 00th January 20xx

DOI: 10.1039/x0xx00000x

www.rsc.org/

Sooyeon Kim,[a] Mamoru Fujitsuka,[a] Norimitsu Tohnai,[b] Takashi Tachikawa,[a,c] Ichiro Hisaki,[b] Mikiji Miyata[a] and Tetsuro Majima*[a]

We report a substitution of 9-phenylanthracenyl group to rhodamine derivatives can induce rhodamine J-aggregate in the aqueous solution upon the addition of halide ion. From X-ray crystallographic analysis, the dramatic red-shift in absorption band (i.e. app. 100 nm) originates from cooperative slipped-stacking of rhodamine and anthracene molecules.

Fluorophore aggregation is an important phenomenon for the design of bio-related fluorescence probes.[1-7] In general, it is considered to be problematic because of fluorescence quenching and reduced water solubility. Thus, many researchers have tried to introduce hydrophilic groups to the probe in order to stay them as a monomer in the aqueous solution. In recent years, aggregate formations are rather intended to develop intriguing traits generated by fluorophore assemblies. For instance, aggregation-induced emission (AIE) gives higher signal-to-noise (S/N) ratio as dye concentration increases and hence is especially suitable for *in vivo* imaging.[4, 6] Furthermore, a formation of aggregates occasionally accompanies a vivid color change, which can be easily detected by the naked eye and advantageous for a practical sensory material.[1, 2, 8]

According to the exciton theory, two interacting molecules can form either blue-shifted and non-fluorescent dimer or red-shifted and fluorescent dimer.[9, 10] The former is called H-aggregate, whereas the latter is assigned to J-aggregate, depending on the values of the angle (ϑ) between the longitudinal axis of the monomer transition moments ($54.7° < \vartheta < 90°$ is H-aggregate, whereas $0° < \vartheta < 54.7°$ is J-aggregate). As mentioned above, it is the H-aggregate formation that causes fluorescence quenching of fluorophores in poor solvent at the high concentration.[11-14] Meanwhile, slipped-stacking-induced J-aggregate of the widely-used fluorophores has been mostly achieved by adsorption on the surface such as glass or zeolite.[15-19] Compared to porphyrin, perylene diimide, and cyanine derivatives that many rational molecular designs have been introduced to induce various aggregation,[20-25] there have been limited reports to control self-assembly of fluorophores in solution without a help of external templates.

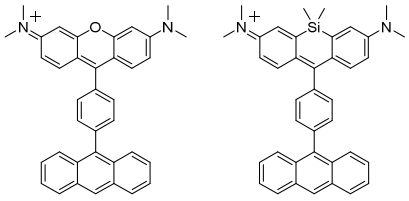

Fig. 1 Chemical structure of **TMR-An** and **SiR-An**.

In this study, we aimed to develop a method to facilitate a J-aggregate formation of fluorophore by substituting a simple chemical group. For this purpose, we focused on a phenylanthracenyl group that can construct diverse crystal structures from the slipped-stacked column to herringbone structures upon the addition of solvent, organic and inorganic salts.[26-28] It was hypothesized that a combination between phenylanthracene and charged fluorophore moieties can trigger unusual fluorophore assemblies apart from the H-dimer, typical aggregates in the aqueous solution. Among various fluorophores, rhodamine derivatives are chosen because of i) their size and planarity similar to anthracene and ii) electron-deficient characteristic as compared to electron-rich anthracene moiety, which further assists the intermolecular interaction. As a consequence, we have found spontaneous J-aggregate formations of tetramethylrhodamine (TMR) and silicon-containing tetramethylrhodamine (Si-TMR) substituted by 9-phenylanthracenyl group, namely **TMR-An** and **SiR-An**, respectively (Fig. 1).

In the aqueous solution, rhodamine derivatives typically form H-aggregate.[11, 12, 14] To our surprise, **TMR-An** and **SiR-An**

[a] *The Institute of Scientific and Industrial Research (SANKEN), Osaka University, Mihogaoka 8-1, Ibaraki, Osaka 567-0047 (Japan).*
[b] *Department of Material and Life Science, Graduate School of Engineering, Osaka University, 2-1 Yamadaoka, Suita, Osaka 565-0871 (Japan).*
[c] *(Current address) Department of Chemistry, Graduate School of Science, Kobe University, 1-1 Rokkodai-cho, Nada-ku, Kobe 657-8501 (Japan).*
E-mail: majima@sanken.osaka-u.ac.jp
† Electronic supplementary information (ESI) available: Experimental details, supporting figures and table. CCDC 1037986.
See DOI: 10.1039/x0xx00000x

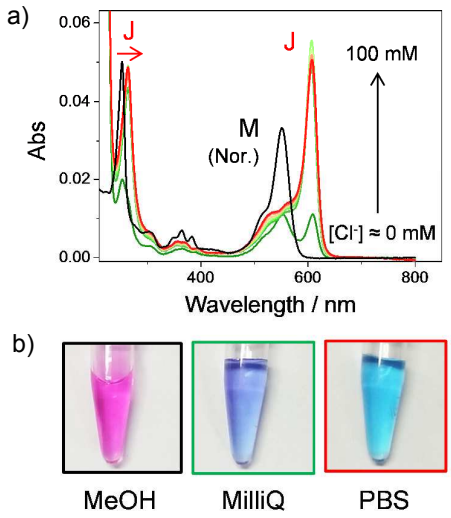

Fig. 2 (a) Normalized absorption spectra of **TMR-An** monomer in methanol (black) and changes in absorption spectra of TMR-An in MilliQ water upon the addition of NaCl from 0 to 100 mM (green to red). M and J indicate the absorption from the monomer and J-aggregates, respectively. [**TMR-An**] = 5 μM, pathlength: 0.2 cm. Black and red arrows show spectral changes reflecting arrangements of TMR and anthracene moieties in a slipped-stacked manner, respectively. (b) Pink to blue colorimetric changes during aggregation of **TMR-An** from a monomer (in methanol) to J-aggregate (MilliQ: [NaCl] ≈ 0 mM; PBS buffer: [NaCl] ≈ 110 mM).

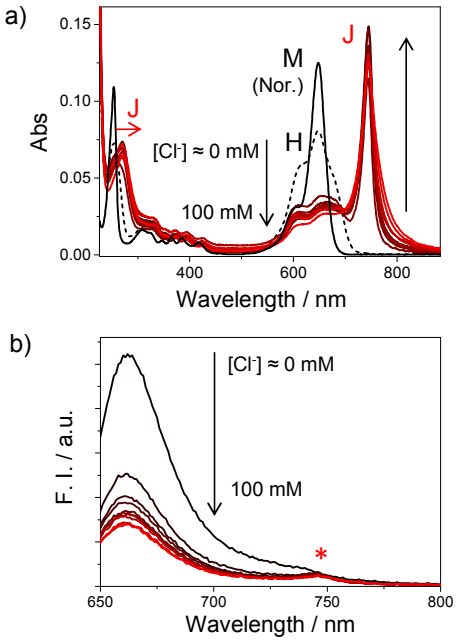

Fig. 3 (a) Normalized absorption spectra of **SiR-An** monomer in methanol (black) and changes in absorption spectra (dashed black line to red) and (b) fluorescence spectra of **SiR-An** in MilliQ water upon the addition of NaCl from 0 to 100 mM (black to red). M, H, and J indicate the absorption from monomer, H- and J-aggregate, respectively. [**SiR-An**] = 5 μM, pathlength: 0.2 cm, λ_{ex} = 640 nm. Black and red arrows show spectral changes reflecting arrangements of Si-TMR and anthracene moieties in a slipped-stacked manner, respectively. A red asterisk indicates emission from Si-TMR J-aggregates.

are found to change their aggregation to J-type upon the addition of NaCl (Fig. 2a and 3a). Especially, λ_{abs} of **TMR-An** is red-shifted approximately 55 nm as **TMR-An** monomers form J-aggregate, accompanying a vivid color change from pink to blue (Fig. 2b). Meanwhile, color of **SiR-An** solutions showed merely slight decoloration (Fig. S4) because λ_{abs} of **SiR-An** is red-shifted approximately 100 nm, leading to the J-band formation in the near-infrared region (Fig. 3a). After 7 days from the sample preparation, blue precipitates were only found for **TMR-An** and **SiR-An** in the PBS solution ([NaCl] ≈ 110 mM) (Fig. S5), indicating the size of aggregates increases spontaneously in the presence of halide ion. Considering together, J-aggregate formations of both compounds are accelerated depending on the concentration of halide ion, while **TMR-An** and **SiR-An** are present as monomer-J-aggregate mixture and H-aggregates, respectively, under the infinitesimal existence of halide ion (green line and black dashed line in Fig. 2a and 3a, respectively).

Unexpectedly, the number of photons emitted (cf. integral of fluorescence intensities at each wavelength) of **TMR-An** and **SiR-An** decreases as more J-aggregate forms (Fig. S6 and 3b). Even though J-aggregate is known to be fluorescent based on the exciton theory,[9, 10] fluorescence of both J-aggregates is negligible (a red asterisk of Fig. 3b). To explain this disagreement, not only the intermolecular interaction among rhodamine moieties, but that between rhodamine and anthracene moieties should be also considered. Indeed, the absorption band of anthracene moieties in **TMR-An** and **SiR-An** both exhibited 11 nm and 16 nm red-shifts, respectively, as [NaCl] increased (Fig. 2a and 3a, respectively). In other words, anthracene moieties in the electronically ground state have interaction with rhodamine moieties, which are making J-coupling at the same time (this is in accordance with the obtained X-ray crystal structure, see Fig. 4). Thus, the fluorescence quenching of **TMR-An** and **SiR-An** J-aggregate presumably originates from ultrafast relaxation of exciton in rhodamine J-aggregates, associated with the intermolecular interaction with anthracene moieties.

In order to reveal a role of a phenylanthracenyl group in the induction of rhodamine J-aggregate, detailed molecular arrangements of rhodamine and anthracene parts in J-aggregates should be clarified. After slow evaporation of methanol solution of **SiR-An**, we could obtain nanocrystal of **SiR-An** and perform X-ray crystallographic analysis. As shown in Fig. 4, Si-TMR and anthracene moieties are slipped-stacked each other, and **SiR-An** stacks are faced to the water layers including chloride (Fig. S7a). In particular, ϑ between the longitudinal axes of two Si-TMR molecules (face-to-face) is determined to be 20.9°, while that between Si-TMR and anthracene moiety (edge-to-face) is 38.9° (Fig. 4b). The X-ray crystallographic and our experimental results are in good agreements with the characteristics of J-aggregate: i) the angle of coplanar inclined transition dipoles (ϑ) is in a range of $0° < \vartheta < 54.7°$; and ii) a sharp red-shifted absorption band with 2–3 nm Stokes shift (Fig. 3).

It is surprising how **SiR-An** can form J-aggregate in the buffer solution, whereas many other Si-TMR derivatives including Si-TMR and dimethylanthracene dyad (cf. Si-DMA that we previously reported as singlet oxygen ($^1O_2$) probe, Fig. S3)[9] undergo only H-aggregate formations under the same condition. We consider such a difference originates from the presence of a central phenyl ring connecting Si-TMR and anthracene moieties which allows cooperative face-to-face and edge-to-face interactions among **SiR-An** molecules (Fig. 4b). As a matter of fact, π-π stacking between two Si-TMR molecules is rather smaller than that between Si-TMR and anthracene moieties (Fig. 4b). The driving force to maintain a slipped-stacked arrangement among Si-TMR moieties is considered to be the π-π interaction between two C-N bonds at the edge of Si-TMR moieties (a blue box in Fig. 4c). Also, CH-π interaction may partly assist this slipped-stacked arrangement (Fig. S7b). Both interactions require that two Si-TMR moieties should be close enough to make π-π interaction. In other words, if a counterion of **SiR-An** is too bulky, such an alignment of **SiR-An** in crystal will be interrupted (Fig. 4). Indeed, bromide and iodide ion could induce J-aggregate of **SiR-An** (Fig. S8), whereas exchanging counteranion to bulkier one such as hexafluorophosphate (PF_6^-) and tetraphenylborate (BPh_4^-) disabled any aggregate formation although hydrophobicity increased by coupling with lipophilic counterions (Fig. S9). On the other hand, J-aggregate formation of **TMR-An** evidences that a dimethyl group in Si-TMR is not the most important factor to induce and maintain slipped-stacking of rhodamine moieties. However, J-aggregate of **TMR-An** probably exhibits less slipped-stacking (presumably, $20.9^\circ < \vartheta < 54.7^\circ$) because of the absence of a dimethyl group in the TMR moiety, resulting in more π-π interaction among TMR moieties than that of **SiR-An**.

From dynamic light scattering (DLS) measurements, we have found there are at least two populations in the size of **SiR-An** J-aggregate regardless of the concentration of **SiR-An**: one in a range of 200–800 nm and another growing up to tens of μm during 2.5 hr incubation (Fig. S10). Nonetheless, in the absence of NaCl or just after the addition of NaCl, the size of **SiR-An** aggregate was undetectable, indicating that the size of H-aggregate is smaller than the detection limit of DLS (i.e. 1–3 nm). Concerning the previous studies on rhodamine aggregates, rhodamine derivatives tend to form antiparallel H-dimer (i.e. directing an opposite side each other) at 10^{-5} M.[29, 30] Particularly, in the case of Si-TMR, a dimethylsilyl group of Si-TMR may interrupt the parallel stacking of Si-TMR molecules (Fig. S11). Overall, in the aqueous solution, **SiR-An** presumably forms antiparallel H-dimer, whereas **SiR-An** J-aggregate (200–800 nm) are formed in the presence of halide ion, and spontaneously gathered together, leading to the secondary aggregates with a loss of J-aggregate characteristics.[31]

Furthermore, **SiR-An** is found to be cell-permeable and reside in mitochondria selectively (Fig. 5). This phenomenon is mostly due to +1 net charge of Si-TMR and appropriate lipophilicity of **SiR-An**, which shares the same mechanism with other Si-TMR derivatives.[11] One interesting aspect is that **SiR-An** must have formed J-aggregate in the culture medium ([Cl^-] ≈ 120 mM), but there was no difference in cell permeability and mitochondria localization between **SiR-An** J-aggregate and Si-DMA H-aggregate. This result strongly implies the possibility of the dyad system composed of fluorophore and phenylanthracene moieties that can be exploited in *in vivo*

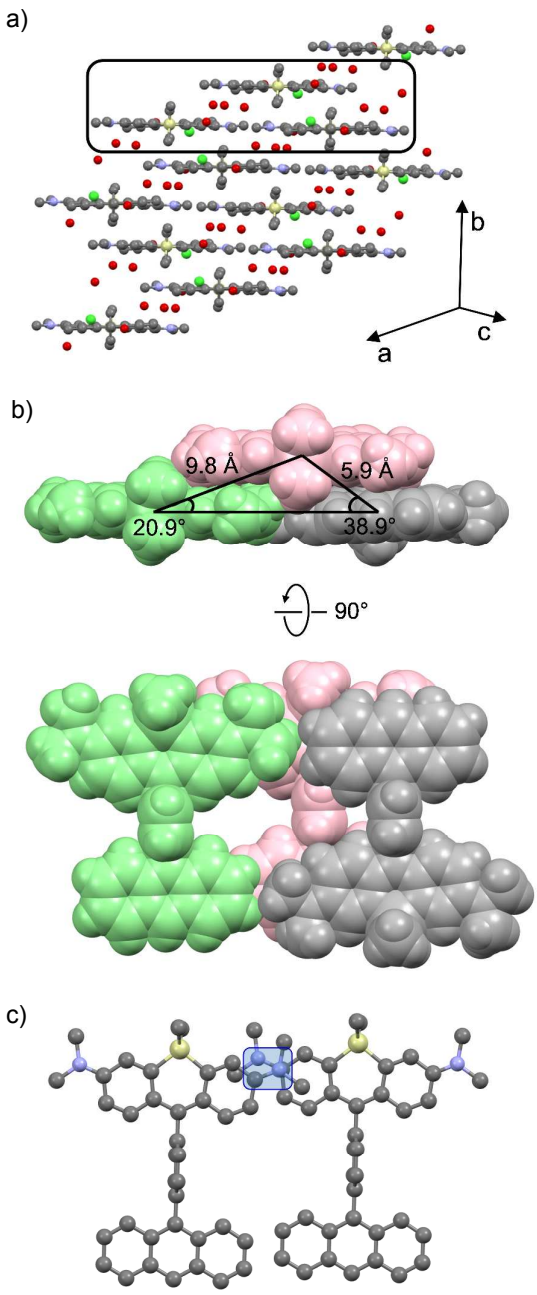

Fig. 4 (a) Extended views of the crystal structure of **SiR-An** aggregate. (b) Geometry of three neighboring **SiR-An** molecules depicted in a black square in Fig. 4a. (c) Plausible π-π interactions between two neighboring Si-TMR moieties of **SiR-An** shown in a blue box. Carbon, silicon, nitrogen atoms, water molecule, and chloride ion are represented in gray, yellow, blue, red, and green, respectively.

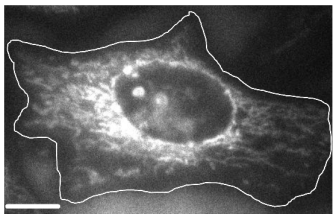

Fig. 5 SiR-An fluorescence image in HeLa cells after incubating with [**SiR-An**] = 100 nM medium for 1 hr. λ_{ex} = 640 nm and scale bar: 10 μm.

imaging in future although the structure is not highly water-soluble.

In this communication, we have designed H- and J-aggregate system of rhodamine derivatives substituted by a 9-phenylanthracenyl group and thoroughly characterized using X-ray crystallography analysis. This study proposes a 9-phenylanthracenyl group as a versatile intramolecular template to align the target fluorophores depending on the presence of organic solvent and counter ions.[26-28] Provided that the fluorophore and anthracene parts are properly modified, this dyad design holds a great potential for sophisticated controlling of the self-assembly of fluorophores, for example, a fluorescence probe with complete fluorescence quenching via intermolecular photoinduced electron transfer, sensitive colorimetric probes, and near-infrared absorbing materials for the energy field application

Furthermore, $^1O_2$ is a particularly important reactive oxygen species in photodynamic therapy and can react with anthracene derivatives, resulting in the endoperoxide formation. Concerning that **SiR-An** exhibited a good cell permeability (Fig. 5), a fluorophore with 9-phenylanthracenyl group suggests a new concept of the cellular $^1O_2$ detection based on the dissociation of fluorophore self-assembly.

We are grateful to Prof. A. Sugimoto for helpful advice on chemical synthesis, P. Zhang for SEM images, A. Kuroda for the preparation of Si-Me, and T. Miyano for the measurement of X-ray crystallography (all belonged to Osaka University). X-ray diffraction data were collected at the BL38B1 in the SPring-8 with approval of JASRI (2014A1252). This work has been partly supported by the Innovative Project for Advanced Instruments, Renovation Center of Instruments for Science Education and Technology, Osaka University, and a Grant-in-Aid for Scientific Research (Projects 25220806, 25288035, and others) from the Ministry of Education, Culture, Sports, Science and Technology (MEXT) of the Japanese Government.

Notes and references

1 Y. Sagara, T. Komatsu, T. Ueno, K. Hanaoka, T. Kato and T. Nagano, *J. Am. Chem. Soc.*, 2014, **136**, 4273-4280.
2 S.-J. Yoon, J. W. Chung, J. Gierschner, K. S. Kim, M.-G. Choi, D. Kim and S. Y. Park, *J. Am. Chem. Soc.*, 2010, **132**, 13675-13683.
3 D. Zhai, W. Xu, L. Zhang and Y.-T. Chang, *Chem. Soc. Rev.*, 2014, **43**, 2402-2411.
4 Y. Hong, J. W. Y. Lam and B. Z. Tang, *Chem. Soc. Rev.*, 2011, **40**, 5361-5388.
5 M. Ogawa, N. Kosaka, P. L. Choyke and H. Kobayashi, *ACS Chem. Biol.,* 2009, **4**, 535-546.
6 Y.-D. Lee, C.-K. Lim, A. Singh, J. Koh, J. Kim, I. C. Kwon and S. Kim, *ACS Nano*, 2012, **6**, 6759-6766.
7 S. Kamino, Y. Horio, S. Komeda, K. Minoura, H. Ichikawa, J. Horigome, A. Tatsumi, S. Kaji, T. Yamaguchi, Y. Usami, S. Hirota, S. Enomoto and Y. Fujita, *Chem. Commun.*, 2010, **46**, 9013-9015.
8 Y. Shirasaki, S. Kamino, M. Tanioka, K. Watanabe, Y. Takeuchi, S. Komeda and S. Enomoto, *Chem.–Asian J.*, 2013, **8**, 2609-2613.
9 M. Kasha, H. R. Rawls and M. Ashraf El-Bayoumi, *Pure Appl. Chem.*, 1965, **11**, 371-592.
10 S. Choi, J. Bouffard and Y. Kim, *Chem. Sci.*, 2014, **5**, 751-755.
11 S. Kim, T. Tachikawa, M. Fujitsuka and T. Majima, *J. Am. Chem. Soc.*, 2014, **136**, 11707-11715.
12 G. Lukinavičius, K. Umezawa, N. Olivier, A. Honigmann, G. Yang, T. Plass, V. Mueller, L. Reymond, I. R. Corrêa, Z. G. Luo, C. Schultz, E. A. Lemke, P. Heppenstall, C. Eggeling, S. Manley and K. Johnsson, *Nat. Chem.*, 2013, **5**, 132-139.
13 K. Sekiguchi, S. Yamaguchi and T. Tahara, *J. Phys. Chem. A*, 2006, **110**, 2601-2606.
14 B. Z. Packard, A. Komoriya, D. D. Toptygin and L. Brand, *J. Phys. Chem. B*, 1997, **101**, 5070-5074.
15 U. Giovanella, G. Leone, G. Ricci, T. Virgili, I. S. Lopez, S. K. Rajendran and C. Botta, *Phys. Chem. Chem. Phys.,* 2012, **14**, 13646-13650.
16 V. Martinez, F. Arbeloa, J. Prieto, T. Lopez and I. Arbeloa, *J. Phys. Chem. B*, 2004, **108**, 20030-20037.
17 F. del Monte and D. Levy, *J. Phys. Chem. B*, 1998, **102**, 8036-8041.
18 M. Busby, C. Blum, M. Tibben, S. Fibikar, G. Calzaferri, V. Subramaniam and L. De Cola, *J. Am. Chem. Soc.*, 2008, **130**, 10970-10976.
19 J. R. Sanchez-Valencia, J. Toudert, L. Gonzalez-Garcia, A. R. Gonzalez-Elipe and A. Barranco, *Chem. Commun.*, 2010, **46**, 4372-4374.
20 F. Würthner, T. E. Kaiser and C. R. Saha-Möller, *Angew. Chem. Int. Ed.*, 2011, **50**, 3376-3410.
21 T. Kobayashi, J. Du and Y. Kida, in *J-Aggregates*, ed. T. Kobayashi, World Scientific, Singapore, 2011, Vol. 2, pp. 1-47.
22 F. Fennel, S. Wolter, Z. Xie, P.-A. Plötz, O. Kühn, F. Würthner and S. Lochbrunner, *J. Am. Chem. Soc.*, 2013, **135**, 18722-18725.
23 D. Ley, C. X. Guzman, K. H. Adolfsson, A. M. Scott and A. B. Braunschweig, *J. Am. Chem. Soc.*, 2014, **136**, 7809-7812.
24 M. Supur and S. Fukuzumi, *ECS J. Solid State Sci. Technol.*, 2013, **2**, M3051-M3062.
25 D. M. Eisele, J. Knoester, S. Kirstein, J. P. Rabe and D. A. Vanden Bout, *Nat. Nanotechnol.*, 2009, **4**, 658-663.
26 T. Hinoue, M. Miyata, I. Hisaki and N. Tohnai, *Angew. Chem. Int. Ed.*, 2012, **51**, 155-158.
27 M. Sugino, K. Hatanaka, Y. Araki, I. Hisaki, M. Miyata and N. Tohnai, *Chem.–Eur. J.*, 2014, **20**, 3069-3076.
28 M. Sugino, K. Hatanaka, T. Miyano, I. Hisaki, M. Miyata, A. Sakon, H. Uekusa and N. Tohnai, *Tetrahedron Lett.*, 2014, **55**, 732-736.
29 R. L. Halterman, J. L. Moore and L. M. Mannel, *J. Org. Chem.*, 2008, **73**, 3266-3269.
30 D. Setiawan, A. Kazaryan, M. A. Martoprawiro and M. Filatov, *Phys. Chem. Chem. Phys.*, 2010, **12**, 11238-11244.
31 A. Li, L. Zhao, J. Hao, R. Ma, Y. An and L. Shi, *Langmuir*, 2014, **30**, 4797-4805.